



Published in final edited form as:

Mol Pharm. 2021 July 05; 18(7): 2657–2668. doi:10.1021/acs.molpharmaceut.1c00189.

Understanding the impact of protein-excipient interactions on physical stability of spray-dried protein solids

Yuan Chen^{1,2}, Jing Ling³, Mingyue Li⁴, Yongchao Su^{1,4}, Kinnari Arte¹, Tarun Mutukuri¹, Lynne S. Taylor¹, Eric J Munson¹, Elizabeth M. Topp^{1,5}, Qi Tony Zhou^{1,*}

¹Department of Industrial and Physical Pharmacy, College of Pharmacy, Purdue University, 575 Stadium Mall Drive, West Lafayette, IN 47907, USA

²Current address: Dosage Form Design & Development, Biopharmaceutical Development, AstraZeneca, 1 MedImmune Way, Gaithersburg, MD 20878, USA

³Discovery Pharmaceutical Sciences, Merck & Co., Inc., South San Francisco, CA 94080, USA

⁴Pharmaceutical Sciences, Merck & Co., Inc, Rahway, NJ 07065, USA

⁵National Institute for Bioprocessing Research and Training, Belfield, Blackrock, Co. Dublin, Ireland A94 X099

Abstract

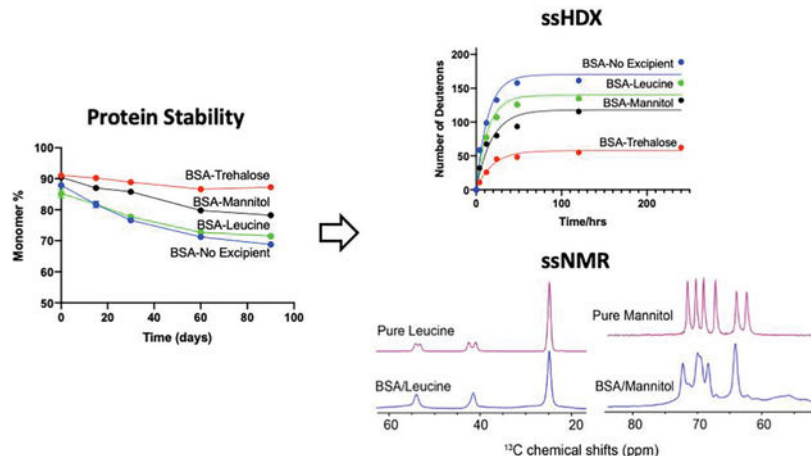
Mannitol, leucine and trehalose have been widely used in spray-dried formulations, especially for inhalation formulations. The individual contribution of these excipients on protein physical stability in spray-dried solids were studied here using bovine serum albumin (BSA) as a model protein. The spray-dried solids were characterized with scanning electron microscopy (SEM), powder X-ray diffraction (PXRD) and solid-state Fourier-transform infrared spectroscopy (ssFTIR) to analyze particle morphology, crystallinity and secondary structure change, respectively. Advanced solid-state characterizations were conducted with solid-state hydrogen-deuterium exchange (ssHDX) and solid-state nuclear magnetic resonance (ssNMR) to explore protein conformation and molecular interactions in the context of the system physical stability. Trehalose remained amorphous after spray drying, and was miscible with BSA, forming hydrogen bonds to maintain protein conformation whereby this system showed the least monomer loss in the stability study. As indicated by ssNMR, both crystalline and amorphous forms of mannitol existed in the spray-dried BSA-mannitol solids, which explained its partial stabilizing effect on BSA. Leucine showed the strongest crystallization tendency after spray drying and did not provide a stabilizing effect due to substantial immiscibility and phase separation with BSA as a result of crystal formation. This work showed novel applications of ssNMR in examining protein conformation and protein-excipient interaction in dry formulations. Overall, our results demonstrate the pivotal role of advanced solid-state characterization techniques in understanding the physical stability of spray-dried protein solids.

*Corresponding Author: Qi (Tony) Zhou, tonyzhou@purdue.edu.

Supporting Information

DSC thermal diagram, ssFTIR spectra, deconvoluted mass spectra (from HDX), and peak area of deconvoluted mass spectra (from HDX) as a function of deuterium incorporation are supplied as Supporting Information.

Graphic Abstract



Keywords

Protein solid; spray drying; excipient; physical stability; molecular interaction

Introduction

Stability is one of the major challenges in the development of pharmaceutical protein products. Compared to small molecules, proteins tend to be subjected to more physical and chemical changes, introducing challenges throughout manufacturing and storage.¹ The larger size of proteins also limits the available routes of administration due to their low permeability across various biological membranes.² Intravenous administration is common for protein products and solution formulations are usually desirable. However, the storage stability of proteins in solutions is often limited.³ Lyophilization has long been utilized in the pharmaceutical industry to manufacture solid dosage forms of biologic products, aiming to preserve protein structure and extend shelf-life.^{4–6} Nevertheless, there are still inevitable disadvantages of lyophilization as a drying technique. For example, the lyophilization drying process is time-consuming and drying efficiency is low.⁷ Lyophilization can take up to several days to achieve a satisfactory moisture content in the product. Additionally, lyophilized solids form a cake in vials as the final dosage form rather than particles/powders. If a particle/powder form is preferred (e.g. for pulmonary delivery), lyophilized solids would require further processing steps such as milling to generate particles,⁸ which in turn could introduce extra mechanical stresses on proteins.^{9, 10} Thus, alternative drying techniques are needed to improve drying efficiency as well as to produce particles that meet certain administration criteria (e.g. for inhalation).

In recent years, spray drying has emerged as a practical drying technique for therapeutic biologics. For instance, spray drying was used to manufacture the inhaled insulin product, Exubera®.¹¹ In 2015, the biological product, Raplixa, produced by aseptic spray drying was approved by US FDA.¹² However, there have been concerns regarding the stability of spray-dried protein solids due to the exposure of protein molecules to thermal and shear

stresses.^{13, 14} For the development of spray-dried protein products, it is crucial to understand stability during drying and upon storage.

Protective excipients are often added to lyophilized protein formulations, and the stabilizing effects of excipients on proteins have been widely studied for lyophilized products.^{15–17} Disaccharide excipients such as sucrose and trehalose are commonly used as lyo-protectants due to their ability to maintain an amorphous solid matrix after lyophilization with reduced molecular mobility, and/or formation of hydrogen bonds with the protein, maintaining the native-state conformation by replacing water.^{4, 18} Spray-dried sucrose formulations tend to crystallize during storage due to low glass transition temperature (T_g) at around 60 °C; trehalose exhibits a much higher T_g value usually above 100 °C,¹⁹ which is preferred in formulations for high-temperature processes such as spray drying.²⁰ In specific products manufactured by spray drying for inhalation, excipients such as mannitol and leucine have been employed, but fundamental understanding of the impact of these excipients, particularly leucine, on the stability of spray-dried protein solids is scarce. Mannitol is among the limited number of excipients that have been used in the FDA-approved inhalation products.²¹ It is generally a bulking excipient in lyophilized protein solids to maintain the cake shape.²² The crystallization of mannitol during lyophilization or spray drying may compromise its capability to stabilize protein solids.^{20, 23–25} Though leucine has not been used in the FDA-approved inhalation products, it has been reported in many studies to enhance the aerosol performance of spray-dried powder formulations for pulmonary delivery.^{26–28} Nevertheless, most previous studies of inhalation formulations focus on the excipient impact on aerosolization rather than stability; there is a need for a mechanistic study of the effects of these excipients on the stability of spray-dried protein solids.

As reported in the previous study, four model proteins including myoglobin, bovine serum albumin, lysozyme and β -lactoglobulin were formulated with sucrose, trehalose or mannitol and processed by either lyophilization or spray drying.²⁰ The storage stability of these solids were studied and correlated with solid-state hydrogen-deuterium exchange (ssHDX) results. The previous study has shown that the lyophilized solids in general have relatively better physical stability compared to the spray-dried solids. ssHDX suggested that spray drying has generated a more heterogeneous solid matrix compared to the lyophilized solids, which could contribute to the protein physical instability.²⁰ In the work reported here, more efforts have been made to understand the individual contribution of mannitol and leucine as the excipients in the spray-dried solids to the protein physical stability. Bovine serum albumin (BSA) was selected as the model protein. BSA has been prepared with each excipient separately as a simplified formulation to understand the correlation between excipient status in spray-dried solids and protein physical stability. Trehalose was used as a stabilizing excipient for comparison and spray-dried BSA without any excipient was included as a negative control.

The spray-dried formulations were characterized using several solid-state characterization techniques to provide information on protein conformation and on the solid matrix. Crystallinity in all the spray-dried BSA solids was initially evaluated using powder X-ray diffraction (PXRD) and changes in the secondary structure of BSA were detected using solid-state Fourier-transform infrared spectroscopy (ssFTIR). ssHDX was applied to study

changes in protein conformation and matrix interactions with higher resolution. In particular, we studied the interactions between excipient and protein in the spray-dried solids using solid-state nuclear magnetic resonance (ssNMR) in the current study. ssNMR has been proved to be a useful technique to examine dynamic information regarding molecular interactions in pharmaceutical solid formulations.^{29, 30} This advanced spectroscopic tool enables high-sensitivity investigation in protein and peptide structures and interactions.^{31, 32} The comprehensive characterization studies facilitated an understanding of the underlying mechanisms in protein stability/instability caused by various excipients.

Materials and Methods

Materials.

Bovine serum albumin (BSA) was purchased from Sigma Aldrich (St. Louis, MO) as a lyophilized powder (98%). D-(+)-Trehalose dihydrate and lithium chloride were obtained from Fisher Scientific (Fair Lawn, NJ). D-mannitol, L-leucine, anhydrous methanol (99.8%), potassium phosphate monobasic, potassium phosphate dibasic, sodium phosphate dibasic heptahydrate and sodium hydroxide were obtained from Sigma Aldrich (St. Louis, MO). Sodium phosphate monobasic was purchased from ACROS Organics (Geel, Belgium). Phosphoric acid (85%, certified ACS), MS-grade water and MS-grade acetonitrile were purchased from Fisher Scientific (Fair Lawn, NJ). Deuterium oxide (D, 99.9%) was obtained from Cambridge Isotope Laboratories, Inc. (Andover, MA). Formic acid (99+%) was purchased from Thermo Scientific (Rockford, IL).

Formulation Preparation.

BSA was dissolved in 2.5 mM potassium phosphate buffer (pH 6.8) and transferred to a dialyzed cassette (Slide-A-Lyzer, 10,000 MWCO, Thermo Scientific, Rockford, IL). BSA stock solution was dialyzed overnight against the same potassium phosphate buffer. Stock solutions of trehalose, D-mannitol and L-leucine were prepared by dissolving each excipient in 2.5 mM potassium phosphate buffer (pH 6.8). The stock solutions of dialyzed BSA and excipient were mixed to reach a total solid concentration of 20 mg/ml with a weight ratio of BSA: excipient of 1:1. For the BSA formulation with no excipient, the stock solution of dialyzed BSA was diluted with the above potassium phosphate buffer to 20 mg/ml. Excipient solutions without BSA were prepared by dissolving excipients (trehalose, D-mannitol or L-Leucine) in 2.5 mM potassium phosphate buffer (pH 6.8) to a solid content of 20 mg/ml. Each solution was filtered using a syringe driven filter unit (0.1 µM, Merck Millipore Ltd., Ireland) prior to spray drying.

Spray Drying Process.

Spray drying process parameters can affect physico-chemical properties and stability of proteins.^{29, 33, 34} The above formulations were spray-dried in a Mini Spray Drier B-290 (BUCHI, New Castle, DE) using methods based on our previous studies.^{20, 35, 36} The inlet temperature was set at 120 °C, allowing the formation of droplets without exposing the protein to extremely high temperature. The resultant outlet temperature was in the range of 60–70 °C. The solution feed rate was 2 ml/min and the air volumetric flow rate was 600 L/min. After collecting the spray-dried powder of each formulation, the powder

was transferred into clear glass vials (2 ml vial, Wheaton, Millville, NJ). The spray-dried samples were further dried in a lyophilizer (REVO[®] Freeze Dryer, Millrock Technology, Kingston, NY) at 30 °C under 100 mTorr for 24 hrs, to minimize the effect of residue moisture on protein stability. Samples were crimped with aluminum seals (13 mm, Wheaton, Millville, NJ) and stored at -20 °C before use.

Moisture Content Measurement.

A 917 KF Coulometer (Metrohm, Riverview, FL) was used to measure the moisture content of the spray-dried samples. Solid samples were reconstituted with anhydrous methanol, the weight of which was recorded. The solution was injected into the coulometer. The weight of the injected solution and the moisture content (in ppm) were recorded and the final results were converted to weight percentage (w/w%). Each formulation was measured in triplicates.

Scanning Electron Microscopy (SEM).

Particle morphology in the solid formulations was visualized using a Teneo VS SEM (FEI Company, Hillsboro, Oregon). Solids were mounted on a specimen stub followed by sputter-coating with platinum for 60 seconds. Images were captured using built-in software at 2kV or 5kV.

Physical Stability by Size Exclusion Chromatography (SEC).

Sealed vials of each formulation were placed in a sealed bag filled with desiccant and stored in an incubator at 40 °C. Samples were collected at 15, 30, 60 and 90 days and reconstituted to reach a protein concentration of 1 mg/ml. Each solution was centrifuged at 12,000 rpm for 10 min at 4°C and the supernatant was transferred to a HPLC vial for analysis. Samples were analyzed using an Agilent 1260 Infinity series HPLC (Santa Clara, CA) with a TOSOH TSKgel[®] G3000SW_{XL} column (7.8 mm I.D. × 30 cm, 5 μm). Protein was eluted over 16 min with a flow of 100 mM sodium phosphate buffer (pH 6.8) at 1 ml/min. HPLC chromatograms were collected with UV at 215 nm.

Solid-state Fourier Transform Infrared Spectroscopy (ssFTIR).

Secondary structures of BSA in the spray-dried solids were measured using a Thermo Nicolet Nexus FTIR (Thermo Scientific, Waltham, MA) equipped with a Smart iTR accessory. Measurements were performed in the attenuated total reflectance mode. Each solid sample was loaded on a flat surface and pressed against the diamond by a metal anvil. The absorbance spectrum was collected from 800 to 4000 cm⁻¹ using 128 scans with a resolution of 4 cm⁻¹. Collected data was processed using the OPUS 6.5 software (Bruker, Billerica, MA) following the steps of baseline-correction, smoothing, normalizing and second derivatization.

X-ray Powder Diffraction (XRPD).

Crystallinity in the spray-dried solids was determined using XRPD (Rigaku SmartLab XRD 600 diffractometer, The Woodlands, Texas, USA) with a Cu K α X-ray source. Each sample was loaded on a glass slide and placed onto the slide-holder. Data was collected from 5° to 40° 2 θ with 0.02 increments.

Glass Transition Temperature (T_g) Measurement.

T_g values of amorphous solid formulations were analyzed by modulated differential scanning calorimetry (MDSC) (DSC 25, TA Instruments, New Castle, DE). Samples were prepared in a glove box with constant nitrogen flow, maintaining the atmospheric moisture content below 10%. Approximately 4 mg of each sample was loaded into a Tzero Pan which was sealed with a Tzero hermetic lid (TA Instruments, New Castle, DE). Samples were heated from 5 °C to 180 °C at 2 °C/min with a modulation period of 60 s and a modulation amplitude of ± 1 °C.

Solid-state Hydrogen-Deuterium Exchange with Mass Spectrometric Analysis (ssHDX-MS).

Saturated LiCl solution in D₂O was placed in a desiccator at room temperature to reach a relative humidity (RH) condition of 11%. Open vials containing solid samples were exposed to D₂O vapor at 11% RH in the desiccator. Approximately 3–5 vials of each formulation were collected from the desiccator at the following time points: 4 h, 12 h, 24 h, 48 h, 120 h and 240 h. To quench the hydrogen-deuterium exchange reaction, samples were immediately immersed into liquid nitrogen and stored at -80 °C until analysis.

Deuterium uptake of BSA in each sample was analyzed using LC-MS (1260 Infinity Series HPLC; 6230 TOF LC/MS; Agilent Technologies, Santa Clara, CA). Solvents were used as following: MS-grade water with 0.1% formic acid (solvent A) and MS-grade acetonitrile with 0.1% formic acid (solvent B). The LC system was connected to a custom-built cooling unit, which was maintained at ~ 1 °C. This unit lowers the temperature of solvent, loops and columns to minimize back exchange in the samples before the protein reaches the MS detector. Ice-cold H₂O (2 ml) containing 0.2% formic acid (pH ~ 2.5) was used to reconstitute the solid sample. An aliquot of 10 μ L solution was injected onto a protein microtrap (Michrom Bioresources, Inc., Auburn, CA). A constant flow of 90% solvent A was run for 2 min to desalt the sample. Protein was eluted over 8 min with a gradient flow from 10% to 90% solvent B. Protein mass was obtained after deconvolution from mass spectra using the MassHunter Workstation Software Version B.07 (Agilent Technologies, Santa Clara, CA).

Kinetics of ssHDX were fitted to a mono-exponential association model using Prism GraphPad software Version 9 (San Diego, CA):

$$D(t) = D_{max}(1 - e^{-kt}) \quad (1)$$

where $D(t)$ is the number of deuterons taken up at a given time t , D_{max} is the maximum deuterium uptake at long D₂O exposure time, and k is the observed first-order rate constant of deuterium incorporation.

Solid-state Nuclear Magnetic Resonance (ssNMR) Spectroscopy Analysis.

Solid-state NMR experiments were carried out using a Bruker Avance III 400 spectrometer (Bruker BioSpin Corporation, Billerica, MA) with ¹H frequency of 400.13 MHz and equipped with a 4 mm H/X probe in the Biopharmaceutical NMR Laboratory (BNL), Pharmaceutical Sciences, MRL at Merck & Co. (West Point, PA). The samples were spun at

12 kHz. ^1H 90° pulse was 3 μs to excite ^1H magnetizations. To transfer the magnetization from ^1H to ^{13}C , the power of ^1H and ^{13}C channels was matched to Hartmann-Hahn condition for cross polarization (CP) transfer. A ramped pulse of 50%–100% was used on the ^1H channel to expand the CP matching condition and the CP contact time was set to 1 ms. High power decoupling of 83.3 kHz on the ^1H channel was applied during data acquisition. 1D ^1H - ^{13}C CP spectra were acquired with 2k number of points of up to 34.4 ms in the direct dimension and averaged with 2k to 8k scans. The corresponding experimental time was between 1 to 4 h. T_1 and $T_{1\rho}$ are the spin-lattice relaxation times in the laboratory and rotating frames, respectively. Considering the time scales of the two relaxation properties, T_1 and $T_{1\rho}$ are often used to evaluate phase separation in solids at the 20–100 nm and 1–20 nm length scales, respectively.³⁰ ^1H T_1 measurements were performed using a saturation recovery sequence with ^{13}C detection. After a ^1H 90° pulse, there is a delay time (τ_1) on the proton channel before CP transfer to ^{13}C for detection. Pseudo 2D experiments with eleven τ delays in the range of 0.5 to 20 s were acquired. $T_{1\rho}$ measurements used a ^1H - ^{13}C CP sequence with a spinlock applied on ^1H after the ^1H 90° pulse for a delay time τ_2 . High spinlock power of 83 kHz was used. Pseudo 2D experiments with an increasing τ_2 delay from 1 ms to 40 ms were acquired.

1D ^{13}C spectra were processed with Fourier Transformation, Gaussian Multiplication, and zero filling. In the ^1H T_1 and $T_{1\rho}$ measurements, integrated peak areas of protein or excipient were plotted as a function of delay times and the T_1 and $T_{1\rho}$ values were obtained by exponential fitting using software TopSpin v3.5. The ^{13}C chemical shift is referenced to the CH_2 group of adamantane at 38.26 ppm. The protein structure in Fig. 6C was generated with UCSF Chimera.³⁷

Results

Moisture Content by Karl Fischer Titration.

The moisture content of all samples was below 1% (Table 1).

Morphology by SEM.

Compared to the lyophilized protein solids, which usually exhibit flake-like sheets,^{38–40} the spray-dried formulations presented as raisin-like wrinkled particles (Fig. 1). Most particles had diameters less than 5 μm , which could be appropriate for inhalation products.^{41, 42} BSA-trehalose particles have a similar morphology to those comprised of BSA without any excipient. BSA-mannitol solids exhibited irregular wrinkled shapes. Particles in the BSA-leucine formulation had donut-like shapes and were less wrinkled than other formulations. Particle sizes were estimated based on SEM images using an open-source sizing software ImageJ developed by National Institute of Health (NIH).^{43, 44} The estimated D50 value was 1.1 μm for the BSA without any excipient, 1.3 μm for the BSA-trehalose, 1.5 μm for the BSA-mannitol and 1.1 μm for the BSA-leucine.

Physical Stability by SEC.

Accelerated stability studies were conducted under 40 $^\circ\text{C}$ incubation for 90 days, and BSA monomer content was recorded (Fig. 2). Before spray drying, the BSA monomer content

in feedstock solution was around 96%. The difference in the monomer content between feedstock and spray-dried solids at $t=0$ could result from the minor loss due to the drying process, which is dependent on the formulation.⁴⁵ For samples at $t=0$, the BSA monomer content in spray-dried solids without any excipient, and with trehalose, mannitol or leucine was: $87.9\pm 0.1\%$, $91.1\pm 0.2\%$, $90.5\pm 0.5\%$ and $85.2\pm 1.4\%$, respectively. At $t=90$ days, the remaining BSA monomer detected in the solids without any excipient, and with trehalose, mannitol or leucine was $68.8\pm 0.1\%$, $87.2\pm 0.3\%$, $78.2\pm 0.5\%$ and $71.5\pm 0.3\%$, respectively. Overall, trehalose was the best protectant, mannitol showed some stabilizing effect, and leucine and excipient-free formulations had the poorest stability in these spray-dried BSA samples.

PXRD and T_g .

The spray-dried BSA samples without any excipient showed no crystalline peak and the BSA-Trehalose solids also exhibited the characteristic amorphous halo (Fig. 3A, B). The BSA-Mannitol solids showed some minor peaks which were difficult to distinguish from background noise (Fig. 3C). Sharp peaks were observed in the BSA-Leucine formulation and the peak positions were consistent with the spray-dried pure leucine (Fig. 3D). Further comparison was performed between the spray-dried BSA formulations with their corresponding excipient reference without BSA (Fig. 3B–D). Spray-dried trehalose was completely amorphous (Fig. 3B). Signature peaks were identified in spray-dried mannitol (Fig. 3C), which were much sharper than those in the BSA-Mannitol formulation. Similarly, peaks corresponding to those in pure leucine were observed in the BSA-Leucine formulation (Fig. 3D).

Based on the PXRD results, T_g values of the spray-dried BSA without any excipient and with trehalose were measured using modulated differential scanning calorimetry (MDSC). The heat flow spectrum of BSA without any excipient did not show a clear transition. T_g of the spray-dried BSA-trehalose solids was $114.0\text{ }^\circ\text{C}$. The thermogram is shown in Fig. S1.

Secondary Structure Change by ssFTIR.

BSA secondary structure primarily consists of α -helix strands spaced by random coils.⁴⁶ In the ssFTIR spectrum, α -helical structure is indicated by bands near 1658 cm^{-1} in the Amide I region.⁴⁷ A perturbation of secondary structure can be indicated by a band position shift and/or an intensity change. ssFTIR spectra of BSA in the spray-dried solids and the as-supplied BSA (i.e., before spray drying) were acquired and the Amide I region is shown in Fig. S2. The FTIR band of BSA in all the formulation solids were observed within the range from 1645 to 1655 cm^{-1} , suggesting retention of the α -helix feature. The band intensity varied among the formulations. The secondary structure of the BSA spray-dried with trehalose exhibited a similar band position and intensity with that in the as-supplied BSA. BSA in trehalose formulation can be considered to be well-preserved since it has been widely used as a stabilizing agent in lyophilized protein formulations.⁴⁸ BSA in the mannitol formulation exhibited a similar band shape and position as those in the trehalose formulation. The band shape was significantly altered for the spray-dried BSA without any excipient, though the solid remained largely amorphous as suggested by PXRD data (Fig. 3A). The secondary structure of the BSA spray-dried with leucine was disrupted

as suggested by the broadening in the FTIR band, consistent with poor stabilization of secondary structure by leucine.

Protein-matrix Interaction Analysis by ssHDX.

Deuterium incorporation by a protein in the solid state on exposure to D₂O vapor can provide information on protein conformational integrity after processing, as well as changes in protein-matrix interactions. Disruption of hydrogen bonding patterns in destabilized proteins may result in a more open conformation or weaker matrix interactions, evidenced by greater incorporation of deuterons. The change in protein conformation can be detected with mass spectrometry by measuring mass increase.⁴⁹ Greater deuterium incorporation has been correlated with higher extent of monomer loss in the storage stability studies.^{20, 50, 51} Excipients in the solid matrix can have stabilizing or destabilizing effects on protein conformation by interacting with it differently. Stabilizing excipients such as disaccharides help to maintain the homogeneous and native protein structure, rendering stable formulations.^{4, 52, 53} The kinetics of deuterium incorporation shows the deuterium uptake over a short time course, which is affected by stabilizing interactions with excipients. The deconvoluted mass spectra of proteins on ssHDX may also reveal protein conformational heterogeneity after spray drying.

The kinetic curves and corresponding parameters of deuterium uptake of the spray-dried solids are shown in Fig. 4 and Table 2. The rank order of D_{max} from high to low was as following: BSA without any excipient > BSA-Leucine > BSA-Mannitol > BSA-Trehalose. BSA in spray-dried solids without any excipient was not protected, showing the highest D_{max} value of deuterium incorporation. The lowest D_{max} value of the BSA-Trehalose formulation is consistent with its greatest stabilizing effect. BSA-Mannitol formulation showed lower D_{max} values than the BSA-Leucine formulation, which led to better stability in the SEC study.

The deconvoluted mass spectra of BSA in spray-dried solids after 240 h of D₂O exposure were examined as an indicator of heterogeneity in protein conformation and/or matrix interactions in the solid samples. Each spectrum was compared to the non-deuterated BSA in solution and the spray-dried BSA without any excipient at the same time point (Fig. S3). The spectrum of the non-deuterated BSA in solution showed the protein conformation with isoforms before spray drying. Without any excipient, greater heterogeneity of BSA was shown after spray drying with peak broadening and merging of isoforms. In the BSA-Trehalose formulation, the peaks of isoforms were distinguishable and peak broadening was less than in BSA without any excipient (Fig. S3 A). Merging of isoform peaks occurred in the mannitol formulation, and the degree of peak broadening was greater than in the trehalose formulation, (Fig. S3 B). The peak shape and width in the leucine formulation are similar to those in the BSA without any excipient, suggesting similar heterogeneity in the protein conformation and environment (Fig. S3 C).

The peak area and deuterium uptake at each time point were normalized against those of the fully deuterated BSA reported previously.²⁰ At the high level of deuterium uptake, (> 30%) peak area values were comparable for BSA without any excipient and the BSA-Leucine formulation, which in turn were greater than those of the BSA-Mannitol formulation (Fig.

S4). In comparing the BSA-Trehalose with the BSA-Mannitol formulations at the same peak area, BSA in the mannitol formulation was more deuterated. This suggests that the conformation and matrix interactions of BSA in the mannitol formulation were more disrupted than in the trehalose formulation even though the proteins were in comparable heterogeneity levels in these two formulations. This also suggests that BSA in the mannitol formulation forms fewer inter- and intramolecular hydrogen bonds and was more exposed to D₂O in the environment than that in the trehalose formulation.

Protein Conformation and Protein-excipient Interactions by ssNMR.

ssNMR was used to further study conformational changes of BSA and phase-separation behavior of the excipients in the spray-dried solids.⁵⁴ Spectral linewidth of NMR can be used to evaluate the conformational homogeneity of proteins while the changes in chemical shifts indicate intermolecular interactions between protein and excipients.⁵⁵ In the spray-dried BSA without any excipient, protein backbone and sidechains including carbonyl, Arg C ξ , aromatic and aliphatic groups can be differentiated according to their unique chemical shifts in a range of 190 to 5 ppm as shown in Fig. 5A. 1D ¹³C spectra of the spray-dried protein solids with or without excipient were acquired and compared with those of pure excipients as references. BSA signals in the absence of excipients showed consistently broader peak patterns than in the spray-dried BSA with excipient (Fig. 5A). The broadened peaks indicate that BSA was amorphous after spray drying with and without any excipient. The crystallization tendencies of the three excipients were compared among the spray-dried formulations. First, the amorphous form of trehalose is consistently identified in both the spray-dried excipient reference and BSA-trehalose sample, highlighting its resistance to recrystallization. On the contrary, sharp NMR peaks of spray-dried pure mannitol suggest its strong tendency to crystallize at ambient conditions. Specifically, recrystallization of mannitol β -form was identified in the pure excipient reference (Fig. 5C).⁵⁶ Broadening of mannitol signals was observed in the BSA-mannitol formulation suggesting the coexistence of amorphous and crystalline forms, in which the α polymorph of mannitol was dominant based on spectral comparison with previous studies.⁵⁶ Leucine displayed comparably narrow linewidth in both the excipient reference and BSA-leucine formulation (Fig. 5B), which is consistent with its crystallinity as shown in the PXRD. The predominantly crystalline signals of leucine suggest its phase separation from the protein component. Interestingly, spray-dried pure leucine showed two sets of C α (54.3 and 53.3 ppm) and C β (42.6 and 41.1 ppm) peaks with almost equal intensity, presumably the result of two crystalline forms after spray-drying. Only one set of C α (54.1 ppm) and C β (41.6 ppm) chemical shifts was found in the spray-dried BSA-leucine solids, indicating that one form becomes dominant when BSA is present.

¹H NMR spin-lattice relaxation measurements have been widely applied to assess the homogeneity of small molecule drugs and excipients in amorphous solid dispersions.^{30, 57–61} The NMR relaxation values in the laboratory (T₁) and rotating frame (T_{1 ρ}) of each component in a mixture reflect the averaged properties of multiple nearby nuclei due to homonuclear spin diffusion. Relaxation parameters on different timescales can be used to evaluate spin diffusion over different length scales. ¹H T₁, typically 1–10 s, corresponds to a spin diffusion over ~ 20–100 nm, while ¹H T_{1 ρ} , ranging from 1–10

ms, estimates spin diffusion over $\sim 1\text{--}20$ nm length scale. With the comparison of $^1\text{H } T_1$ and $T_{1\rho}$ of both protein and excipient, mixing of two components can be estimated on large and small scales in nanometer range. There would be three possible conditions: (1) comparable T_1 and $T_{1\rho}$ between both components indicates homogeneity; (2) comparable $^1\text{H } T_1$ but different $^1\text{H } T_{1\rho}$ indicates that two components are relatively homogeneous at the 20–100 nm scale but non-homogeneous at the 1–20 nm scale; (3) both $^1\text{H } T_1$ and $^1\text{H } T_{1\rho}$ are different, suggesting phase separation at a scale greater than 20–100 nm.

^1H relaxation parameters (Table 3) were used to analyze the homogeneity of BSA and excipient in spray-dried samples. Since leucine showed a strong crystallization tendency in the BSA formulation it was not included in the analysis. The BSA-trehalose formulation showed homogeneity at both 20–100 nm and 1–20 nm scales as indicated by comparable $^1\text{H } T_1$ and $^1\text{H } T_{1\rho}$ values between BSA and trehalose. This is expected, as trehalose is an excellent stabilizer for BSA. Due to the coexistence of crystalline and amorphous forms of mannitol, $^1\text{H } T_1$ curve of the BSA-mannitol formulation was modeled as a two-component system, with a calculated relaxation time of with 15.94 s corresponding to the crystalline form and 2.79 s to the amorphous form. Mannitol crystallization after spray drying was expected considering its strong tendency to crystallize.⁶² The $^1\text{H } T_1$ of the crystalline mannitol was significant different from that of the BSA, confirming phase separation at the 20–100 nm scale, as would be expected for a crystalline excipient. At the same time, the amorphous mannitol is homogeneously mixed with BSA at the 20–100 nm scale. The $^1\text{H } T_{1\rho}$ was significantly different between BSA and amorphous mannitol, suggesting a lack of homogeneity at the 1–20 nm length scale. Part of mannitol were homogeneously mixed with BSA on a large length scale. Inhomogeneous domains of mannitol and BSA formed on the smaller length scale. These homogeneously mixed domains would differ in the ratio of mannitol and BSA on a local location. This has been observed in drug-polymer systems when the polymer level is relatively low compared to the drug level, indicating that the excess drug is not homogeneously mixed with the polymer. Such microstructures containing both homogeneous and inhomogeneous mixtures of excipient and drug contributes to physical stability and drug release.⁶¹ Notably, the $^1\text{H } T_1$ of BSA increased in the order of BSA without excipient < BSA-mannitol < BSA-trehalose. Longer relaxation times are an indicator of lower molecular mobility in lyophilized protein formulations, and usually correspond to better stability.^{63, 64} The results indicate that the molecular motion of BSA was hindered by the presence of trehalose molecules in a homogeneous mixture due to lower molecular mobility, and/or potential intermolecular interactions.^{65–67}

The impact of sugar excipients on the BSA conformational distribution and potential intermolecular interactions was further investigated. A larger peak width in the NMR spectrum is usually indicative of a broader conformational distribution and/or dynamic disorders.⁶⁸ BSA in trehalose and mannitol formulations both showed decreased linewidth as compared to BSA without any excipient (Fig. 6A, Table 3). This indicates that the higher energy conformations for BSA were not present in the presence of the excipients, although susceptibility broadening may also play a role, as the presence of excipients can result in a narrower line width for inhomogeneously-broadened lines. Moreover, as shown in Fig. 6C, Arg sidechain -NH and -NH₂ are largely involved in hydrogen bonding as H-donors to maintain the helical structure and tertiary folding of BSA. At ~ 157 ppm assigned to

sidechain C ξ of Arg, the signal in mannitol and trehalose formulations was shifted from that of BSA without any excipient (Fig. 6B). One possible explanation is the disruption of intramolecular hydrogen bonds in BSA and possible formation of new intermolecular bonds with sugar molecules⁴⁸ and can be explored further by using multidimensional ssNMR experiments.^{69, 70}

Discussion

Spray drying is a promising drying method for biologics due to high drying efficiency as well as controlled particle characteristics such as size and shape. The spray drying process is considered to be intrinsically more aggressive than lyophilization, as molecules are exposed to hot gas through evaporation and to various interface and shear stresses, all of which may disrupt protein conformation and decrease stability during storage.^{13, 29, 71} Adding excipients to lyophilized formulations can effectively stabilize many proteins solids.⁵ However, the systemic examinations of excipient effects on protein stability in spray-dried solids is limited. It is critical to have a better understanding of the relationship between protein-matrix interactions and storage stability for the spray-dried solids.

Disaccharides are considered to be stabilizing excipients for their ability to form direct hydrogen bonds with proteins in solid to stabilize their structure, and/or maintain amorphous state to reduce matrix mobility.^{4, 18} Here, the solid matrix remained amorphous in the BSA-Trehalose formulation (Fig. 3B) and the secondary structure of BSA was well preserved as compared to that in the spray-dried BSA without any excipient (Fig. S2). Crystalline peaks of leucine were observed in PXRD data (Fig. 3D) and the secondary structure of BSA in the leucine formulation was disrupted (Fig. S2). Phase separation between amorphous BSA and crystalline leucine in the BSA-Leucine formulation was observed and may have contributed to the decreased protective interactions between BSA and leucine, which resulted in low monomer level by in the stability study (Fig. 2). For the spray-dried BSA-Mannitol solids, ssFTIR suggested that the secondary structure of BSA was well preserved (Fig. S2) while crystallization of mannitol cannot be completely determined by PXRD (Fig. 3C). However, in stability studies, mannitol did not stabilize BSA in spray-dried solids to the same extent as trehalose (Fig. 2).

A more detailed understanding of protein conformation and interactions in the solid matrix in the various BSA formulations was achieved with ssHDX and ssNMR. As suggested by the D_{\max} value from the kinetics of ssHDX, the conformation of BSA was preserved in the order of trehalose > mannitol > leucine > no excipient (Table 2). Similar results were obtained in the reduced carbonyl linewidth of BSA in the BSA-Trehalose formulation and the BSA-Mannitol formulation (Table 3). With no excipient, the intra- and intermolecular interactions in BSA solids were disrupted, leading to a more heterogeneous protein conformation (Fig. S3 and S4). Trehalose may interact with BSA through hydrogen bonding, thereby preserving protein conformation and enhancing stability (Fig. S3 and S4). The direct interaction between BSA and leucine could be hardly observed (Table 2, Fig. S3 C) and the stabilizing effect of leucine was negligible (Fig. 2), observations that may reflect phase separation of the protein and the crystalline formation of leucine in the solid matrix (Fig. 3D). As suggested by the 1D ¹H-¹³C cross-polarization spectra (Fig. 5 B), one

dominant form of crystalline leucine existed in the spray-dried solids with the existence of BSA, while two forms of crystalline leucine were almost equally detected without BSA, demonstrating that the presence of the protein has affected the crystal form of leucine.

Mannitol in the spray-dried formulation provided a partial protective effect, which differed from both trehalose and leucine. The ssNMR study provided some fundamental understanding regarding the behavior of mannitol. The solid matrix formed by mannitol was a mixture of an amorphous form and a crystalline form (Fig. 5C, Table 3). The crystalline form of mannitol was phase-separated from BSA at both 20–100 nm and 1–20 nm scales, while its amorphous form was miscible with BSA at 20–100 nm but phase-separated at 1–20 nm (Table 3). Mannitol, particularly the amorphous mannitol in the solid matrix, formed some hydrogen bonds to stabilize BSA, and Arg was identified as an important H-bond donor (Fig. 6C). The chemical shifts of Arg C ξ peaks were comparable in the mannitol and trehalose formulations, suggesting that they could have interacted with BSA in similar hydrogen bonding patterns. However, phase-separation due to immiscibility between the amorphous BSA and the crystalline mannitol disrupted the protein conformation somewhat, as evidenced by higher levels of deuterium uptake than in the trehalose formulation (Fig. S3 A and B, Fig. S4).

It is worth noting that the PXRD crystalline peaks of spray-dried pure mannitol were much stronger and sharper than those of mannitol in the BSA-Mannitol formulation (Fig. 3), suggesting that BSA suppressed the crystallization tendency of mannitol. In a study of a lyophilized monoclonal antibody (mAb) formulation, crystallization of mannitol in protein solids was related to protein concentration.⁷² With 5% (w/w) of mannitol in solution before lyophilization, the effect of the mAb on inhibiting mannitol crystallization was observed at 20 mg/ml, and enhanced when the concentration increased from 30 to 50 mg/ml, as suggested by the change in glass transition temperature of the maximally freeze-concentrated amorphous phase (T_g).⁷² Here, the presence of BSA in the formulation generated different polymorphs of mannitol after spray drying (Fig. 3C, Fig. 5C). Briefly, the relatively sharp ¹³C NMR peaks of mannitol are retained in the spray dried sample (Fig. 5C: bottom) but peak positions differ from the pure crystalline mannitol reference (Fig. 5C: top). A similar observation was reported previously for spray-dried anti-IgE mAb solids containing different concentrations of mannitol, in which the peak patterns of pure mannitol from PXRD differed from those of solids containing the mAb.⁷³ These studies suggest that protein in the formulation not only suppresses the crystallization tendency of mannitol, but also influence the specific polymorphs of mannitol that are formed during spray drying. Future study is warranted to examine the interactions between protein and mannitol with varying mannitol concentrations, and their impact on protein stability.

For the purpose of inhalation, the aerosol performance of spray-dried solids should be considered in the formulation design. Disaccharide excipients such as trehalose are hygroscopic, and can be sensitive to changes in environmental moisture which in turn can negatively affect the aerosol performance. It has been reported that leucine can improve the aerosol performance^{74, 75} and alleviate moisture-reduced aerosolization of spray-dried formulations.^{76, 77} However, leucine tends to crystallize and consequently provides a negligible stabilizing effect to proteins in spray-dried solids during storage. Thus, both

protein stability and aerosol performance should be considered when designing formulations for inhalation. A further study of on combined excipients of trehalose and leucine in the spray-dried protein formulations is warranted.

Conclusions

This study aimed to understand how the excipient status of mannitol and leucine contribute to protein stability in spray-dried solids. The protein conformation difference measured by ssHDX in the spray-dried solids correlated well with their physical stability on storage as measured by SEC. In particular, ssNMR data further revealed that the immiscibility of BSA with the crystallized excipients of mannitol and leucine in the solid contributed to the instability. Trehalose remained amorphous after spray drying, formed hydrogen bonds with BSA, and showed the best protection of stability for BSA among the three excipients studied. The solid matrix of mannitol was partially amorphous, and crystallization of mannitol apparently decreased its ability to stabilize the protein. Leucine substantially crystallized after spray drying and phase-separated from BSA, and had a negligible stabilizing effect. This study has provided a fundamental molecular understanding on the effects of various excipients in spray-dried protein solids using advanced solid-state characterization techniques such as ssHDX and ssNMR.

Supplementary Material

Refer to Web version on PubMed Central for supplementary material.

Acknowledgement

This study was partially supported by a grant from Merck & Co., Inc. Qi (Tony) Zhou and Yuan Chen were supported by the National Institute of Allergy and Infectious Diseases of the National Institute of Health (NIH) under Award Number R01AI146160. The content is solely the responsibility of the authors and does not necessarily represent the official views of the NIH.

References

1. Krishnamurthy R; Manning MC The stability factor: importance in formulation development. *Current pharmaceutical biotechnology* 2002, 3, (4), 361–371. [PubMed: 12463418]
2. Frokjaer S; Otzen DE Protein drug stability: a formulation challenge. *Nature reviews drug discovery* 2005, 4, (4), 298–306. [PubMed: 15803194]
3. Chi EY; Krishnan S; Randolph TW; Carpenter JF Physical stability of proteins in aqueous solution: mechanism and driving forces in nonnative protein aggregation. *Pharmaceutical research* 2003, 20, (9), 1325–1336. [PubMed: 14567625]
4. Wang W Lyophilization and development of solid protein pharmaceuticals. *International journal of pharmaceutics* 2000, 203, (1–2), 1–60. [PubMed: 10967427]
5. Carpenter JF; Pikal MJ; Chang BS; Randolph TW Rational design of stable lyophilized protein formulations: some practical advice. *Pharmaceutical research* 1997, 14, (8), 969–975. [PubMed: 9279875]
6. Garidel P; Presser I, Lyophilization of high-concentration protein formulations. In *Lyophilization of Pharmaceuticals and Biologicals*, Springer: 2019; pp 291–325.
7. Rey L, *Freeze-drying/lyophilization of pharmaceutical and biological products*. CRC Press: 2016.
8. Shoyele SA; Cawthorne S Particle engineering techniques for inhaled biopharmaceuticals. *Advanced drug delivery reviews* 2006, 58, (9–10), 1009–1029. [PubMed: 17005293]

9. Amorij JP; Huckriede A; Wilschut J; Frijlink HW; Hinrichs WLJ Development of stable influenza vaccine powder formulations: challenges and possibilities. *Pharmaceutical research* 2008, 25, (6), 1256–1273. [PubMed: 18338241]
10. Desai TR; Wong JP; Hancock REW; Finlay WH A novel approach to the pulmonary delivery of liposomes in dry powder form to eliminate the deleterious effects of milling. *Journal of pharmaceutical sciences* 2002, 91, (2), 482–491. [PubMed: 11835207]
11. White S; Bennett DB; Cheu S; Conley PW; Guzek DB; Gray S; Howard J; Malcolmson R; Parker JM; Roberts P EXUBERA[®]: pharmaceutical development of a novel product for pulmonary delivery of insulin. *Diabetes technology & therapeutics* 2005, 7, (6), 896–906. [PubMed: 16386095]
12. Costa S. d. Raplixa case study: Enabling an innovative drug presentation through aseptic spray drying. *Pharmaceutical Technology* 2016, 40, (7), 26.
13. Ameri M; Maa Y-F Spray drying of biopharmaceuticals: stability and process considerations. *Drying technology* 2006, 24, (6), 763–768.
14. Cal K; Sollohub K Spray drying technique. I: Hardware and process parameters. *Journal of pharmaceutical sciences* 2010, 99, (2), 575–586. [PubMed: 19774644]
15. Lai MC; Topp EM Solid-state chemical stability of proteins and peptides. *Journal of pharmaceutical sciences* 1999, 88, (5), 489–500. [PubMed: 10229638]
16. Chang L; Pikal MJ Mechanisms of protein stabilization in the solid state. *Journal of Pharmaceutical Sciences* 2009, 98, (9), 2886–2908. [PubMed: 19569054]
17. Carpenter JF; Prestrelski SJ; Anchordoguy TJ; Arakawa T, Interactions of Stabilizers with Proteins During Freezing and Drying. In *Formulation and Delivery of Proteins and Peptides*, American Chemical Society: 1994; Vol. 567, pp 134–147.
18. Crowe JH; Carpenter JF; Crowe LM The role of vitrification in anhydrobiosis. *Annual review of physiology* 1998, 60, (1), 73–103.
19. Simperler A; Kornherr A; Chopra R; Bonnet PA; Jones W; Motherwell WDS; Zifferer G Glass transition temperature of glucose, sucrose, and trehalose: an experimental and in silico study. *The Journal of Physical Chemistry B* 2006, 110, (39), 19678–19684. [PubMed: 17004837]
20. Wilson NE; Topp EM; Zhou QT Effects of drying method and excipient on structure and stability of protein solids using solid-state hydrogen/deuterium exchange mass spectrometry (ssHDX-MS). *International Journal of Pharmaceutics* 2019, 567, 118470. [PubMed: 31252148]
21. Hertel N; Birk G; Scherließ R Particle engineered mannitol for carrier-based inhalation—A serious alternative? *International Journal of Pharmaceutics* 2020, 577, 118901. [PubMed: 31846726]
22. Kim AI; Akers MJ; Nail SL The physical state of mannitol after freeze-drying: effects of mannitol concentration, freezing rate, and a noncrystallizing cosolute. *Journal of pharmaceutical sciences* 1998, 87, (8), 931–935. [PubMed: 9687336]
23. Liao X; Krishnamurthy R; Suryanarayanan R. J. P. r. Influence of the active pharmaceutical ingredient concentration on the physical state of mannitol—implications in freeze-drying. 2005, 22, (11), 1978–1985.
24. Costantino HR; Andya JD; Nguyen PA; Dasovich N; Sweeney TD; Shire SJ; Hsu CC; Maa Y. F. J. J. o. p. s. Effect of mannitol crystallization on the stability and aerosol performance of a spray-dried pharmaceutical protein, recombinant humanized anti-IgE monoclonal antibody. 1998, 87, (11), 1406–1411.
25. Andya JD; Maa Y-F; Costantino HR; Nguyen P-A; Dasovich N; Sweeney TD; Hsu CC; Shire SJ J. P. r. The effect of formulation excipients on protein stability and aerosol performance of spray-dried powders of a recombinant humanized anti-IgE monoclonal antibody1. 1999, 16, (3), 350–358.
26. Li L; Sun S; Parumasivam T; Denman JA; Gengenbach T; Tang P; Mao S; Chan H-K l-Leucine as an excipient against moisture on in vitro aerosolization performances of highly hygroscopic spray-dried powders. *European Journal of Pharmaceutics and Biopharmaceutics* 2016, 102, 132–141. [PubMed: 26970252]
27. Aquino RP; Protá L; Auriemma G; Santoro A; Mencherini T; Colombo G; Russo P Dry powder inhalers of gentamicin and leucine: formulation parameters, aerosol performance and in

- vitro toxicity on CuFi1 cells. *International journal of pharmaceutics* 2012, 426, (1–2), 100–107. [PubMed: 22301426]
28. Chow MYT; Qiu Y; Lo FFK; Lin HHS; Chan H-K; Kwok PCL; Lam JKW Inhaled powder formulation of naked siRNA using spray drying technology with L-leucine as dispersion enhancer. *International journal of pharmaceutics* 2017, 530, (1–2), 40–52. [PubMed: 28720537]
 29. Chen Y; Mutukuri TT; Wilson NE; Zhou Q Pharmaceutical protein solids: Drying technology, solid-state characterization and stability. *Advanced Drug Delivery Reviews* 2021, 172, 211–233. [PubMed: 33705880]
 30. Li M; Xu W; Su Y Solid-state NMR Spectroscopy in Pharmaceutical Sciences. *TrAC Trends in Analytical Chemistry* 2020, 116152.
 31. Hong M; Su Y Structure and dynamics of cationic membrane peptides and proteins: Insights from solid-state NMR. *J Protein Science* 2011, 20, (4), 641–655.
 32. Su Y; Andreas L; Griffin R Magic angle spinning NMR of proteins: high-frequency dynamic nuclear polarization and 1H detection. *J Annual review of biochemistry* 2015, 84, 465–497.
 33. Brunaugh AD; Wu T; Kanapuram SR; Smyth HDC Effect of Particle Formation Process on Characteristics and Aerosol Performance of Respirable Protein Powders. *Molecular Pharmaceutics* 2019, 16, (10), 4165–4180. [PubMed: 31448924]
 34. Ferrati S; Wu T; Fuentes O; Brunaugh AD; Kanapuram SR; Smyth HDC. Influence of formulation factors on the aerosol performance and stability of lysozyme powders: A systematic approach. *AAPS PharmSciTech* 2018, 19, (7), 2755–2766. [PubMed: 29488193]
 35. Mutukuri TT; Wilson NE; Taylor LS; Topp EM; Zhou QT Effects of drying method and excipient on the structure and physical stability of protein solids: Freeze drying vs. spray freeze drying. *International Journal of Pharmaceutics* 2021, 594, 120169. [PubMed: 33333176]
 36. Wilson NE; Mutukuri TT; Zemlyanov DY; Taylor LS; Topp EM; Zhou QT Surface Composition and Formulation Heterogeneity of Protein Solids Produced by Spray Drying. *Pharmaceutical Research* 2020, 37, (1), 14.
 37. Pettersen EF; Goddard TD; Huang CC; Couch GS; Greenblatt DM; Meng EC; Ferrin TE UCSF Chimera—a visualization system for exploratory research and analysis. *Journal of computational chemistry* 2004, 25, (13), 1605–1612. [PubMed: 15264254]
 38. Haque MK; Roos YH Differences in the physical state and thermal behavior of spray-dried and freeze-dried lactose and lactose/protein mixtures. *Innovative Food Science & Emerging Technologies* 2006, 7, (1), 62–73.
 39. Fäldt P; Bergenstahl B The surface composition of spray-dried protein—lactose powders. *Colloids and Surfaces A: Physicochemical and Engineering Aspects* 1994, 90, (2), 183–190.
 40. Webb SD; Cleland JL; Carpenter JF; Randolph TW Effects of annealing lyophilized and spray-lyophilized formulations of recombinant human interferon- γ . *Journal of Pharmaceutical Sciences* 2003, 92, (4), 715–729. [PubMed: 12661058]
 41. Patton JS; Byron PR Inhaling medicines: delivering drugs to the body through the lungs. *Nature Reviews Drug Discovery* 2007, 6, (1), 67–74. [PubMed: 17195033]
 42. Glover W; Chan H-K; Eberl S; Daviskas E; Verschuer J Effect of particle size of dry powder mannitol on the lung deposition in healthy volunteers. *International Journal of Pharmaceutics* 2008, 349, (1), 314–322. [PubMed: 17904774]
 43. Schneider CA; Rasband WS; Eliceiri KW NIH Image to ImageJ: 25 years of image analysis. *Nature Methods* 2012, 9, (7), 671–675. [PubMed: 22930834]
 44. Shetty N; Ahn P; Park H; Bhujbal S; Zemlyanov D; Cavallaro A; Mangal S; Li J; Zhou QT Improved physical stability and aerosolization of inhalable amorphous ciprofloxacin powder formulations by incorporating synergistic colistin. *Molecular pharmaceutics* 2018, 15, (9), 4004–4020. [PubMed: 30028947]
 45. Rajagopal K; Wood J; Tran B; Patapoff TW; Nivaggioli T. J. J. o. p. s. Trehalose limits BSA aggregation in spray-dried formulations at high temperatures: implications in preparing polymer implants for long-term protein delivery. 2013, 102, (8), 2655–2666.
 46. Bujacz A Structures of bovine, equine and leporine serum albumin. *Acta Crystallographica Section D: Biological Crystallography* 2012, 68, (10), 1278–1289. [PubMed: 22993082]

47. Fu K; Griebenow K; Hsieh L; Klibanov AM; Robert L FTIR characterization of the secondary structure of proteins encapsulated within PLGA microspheres | An article of related interest has been published by Yang et al. in *J. Pharm. Sci.*, 88(2), Feb. 1999, accepted Nov. 1998.1. *Journal of Controlled Release* 1999, 58, (3), 357–366. [PubMed: 10099160]
48. Mensink MA; Frijlink HW; van der Voort Maarschalk K.; Hinrichs WLJ. How sugars protect proteins in the solid state and during drying (review): Mechanisms of stabilization in relation to stress conditions. *European Journal of Pharmaceutics and Biopharmaceutics* 2017, 114, 288–295. [PubMed: 28189621]
49. Sophocleous AM; Topp EM Localized Hydration in Lyophilized Myoglobin by Hydrogen–Deuterium Exchange Mass Spectrometry. 2. Exchange Kinetics. *Molecular pharmaceutics* 2012, 9, (4), 727–733. [PubMed: 22352990]
50. Moorthy BS; Schultz SG; Kim SG; Topp EM Predicting Protein Aggregation during Storage in Lyophilized Solids Using Solid State Amide Hydrogen/Deuterium Exchange with Mass Spectrometric Analysis (ssHDX-MS). *Molecular Pharmaceutics* 2014, 11, (6), 1869–1879. [PubMed: 24816133]
51. Moussa EM; Wilson NE; Zhou QT; Singh SK; Nema S; Topp EM Effects of Drying Process on an IgG1 Monoclonal Antibody Using Solid-State Hydrogen/Deuterium Exchange with Mass Spectrometric Analysis (ssHDX-MS). *Pharmaceutical Research* 2018, 35, (1), 12. [PubMed: 29299701]
52. Costantino HR; Carrasquillo KG; Cordero RA; Mumenthaler M; Hsu CC; Griebenow K Effect of excipients on the stability and structure of lyophilized recombinant human growth hormone. *Journal of pharmaceutical sciences* 1998, 87, (11), 1412–1420. [PubMed: 9811499]
53. Allison SD; Chang B; Randolph TW; Carpenter JF Hydrogen bonding between sugar and protein is responsible for inhibition of dehydration-induced protein unfolding. *Archives of Biochemistry and Biophysics* 1999, 365, (2), 289–298. [PubMed: 10328824]
54. Mensink MA; Nethercott MJ; Hinrichs WL; van der Voort Maarschalk K.; Frijlink HW; Munson EJ.; Pikal M. J. J. T. A. j. Influence of miscibility of protein-sugar lyophilizates on their storage stability. 2016, 18, (5), 1225–1232.
55. Martin RW; Zilm KW Preparation of protein nanocrystals and their characterization by solid state NMR. *J Magn Reson* 2003, 165, (1), 162–174. [PubMed: 14568526]
56. Grindley TB; Mckinnon MS; Wasylshen RE Towards Understanding C-13-Nmr Chemical-Shifts of Carbohydrates in the Solid-State - the Spectra of D-Mannitol Polymorphs and of DI-Mannitol. *Carbohydr Res* 1990, 197, 41–52.
57. Hanada M; Jermain SV; Lu XY; Su YC; Williams RO Predicting physical stability of ternary amorphous solid dispersions using specific mechanical energy in a hot melt extrusion process. *International Journal of Pharmaceutics* 2018, 548, (1), 571–585. [PubMed: 30006310]
58. Paudel A; Geppi M; Mooter GVD Structural and dynamic properties of amorphous solid dispersions: the role of solid-state nuclear magnetic resonance spectroscopy and relaxometry. *J Pharm Sci* 2014, 103, (9), 2635–2662. [PubMed: 24715618]
59. Purohit HS; Ormes JD; Saboo S; Su Y; Lamm MS; Mann AKP; Taylor LS Insights into Nano- and Micron-Scale Phase Separation in Amorphous Solid Dispersions Using Fluorescence-Based Techniques in Combination with Solid State Nuclear Magnetic Resonance Spectroscopy. *Pharm Res* 2017, 34, (7), 1364–1377. [PubMed: 28455777]
60. Li M; Koranne S; Fang R; Lu X; Williams DM; Munson EJ; Bhambhani A; Su Y Probing Microenvironmental Acidity in Lyophilized Protein and Vaccine Formulations Using Solid-state NMR Spectroscopy. *Journal of Pharmaceutical Sciences* 2020.
61. Duan P; Lamm MS; Yang F; Xu W; Skomski D; Su Y; Schmidt-Rohr K Quantifying Molecular Mixing and Heterogeneity in Pharmaceutical Dispersions at Sub-100 nm Resolution by Spin Diffusion NMR. *Molecular Pharmaceutics* 2020, 17, (9), 3567–3580. [PubMed: 32787281]
62. Telang C; Yu L; Suryanarayanan R Effective inhibition of mannitol crystallization in frozen solutions by sodium chloride. *Pharm Res* 2003, 20, (4), 660–7. [PubMed: 12739776]
63. Yoshioka S; Aso Y; Kojima S Different molecular motions in lyophilized protein formulations as determined by laboratory and rotating frame spin-lattice relaxation times. *Journal of Pharmaceutical Sciences* 2002, 91, (10), 2203–2210. [PubMed: 12226847]

64. Lam YH; Bustami R; Phan T; Chan HK; Separovic F A solid-state NMR study of protein mobility in lyophilized protein-sugar powders. *Journal of Pharmaceutical Sciences* 2002, 91, (4), 943–951. [PubMed: 11948532]
65. Tonnis WF; Mensink MA; de Jager A; Maarschalk KV; Frijlink HW; Hinrichs WLJ Size and Molecular Flexibility of Sugars Determine the Storage Stability of Freeze-Dried Proteins. *Molecular Pharmaceutics* 2015, 12, (3), 684–694. [PubMed: 25581526]
66. Mensink MA; Frijlink HW; Maarschalk KV; Hinrichs WLJ How sugars protect proteins in the solid state and during drying (review): Mechanisms of stabilization in relation to stress conditions. *European Journal of Pharmaceutics and Biopharmaceutics* 2017, 114, 288–295. [PubMed: 28189621]
67. Yuan X; Sperger D; Munson EJ Investigating miscibility and molecular mobility of nifedipine-PVP amorphous solid dispersions using solid-state NMR spectroscopy. *Molecular pharmaceutics* 2014, 11, (1), 329–337.
68. Su Y; Hong M Conformational Disorder of Membrane Peptides Investigated from Solid-State NMR Line Widths and Line Shapes. *The Journal of Physical Chemistry B* 2011, 115, (36), 10758–10767. [PubMed: 21806038]
69. Lu X; Huang C; Lowinger MB; Yang F; Xu W; Brown CD; Hesk D; Koynov A; Schenck L; Su Y Molecular Interactions in Posaconazole Amorphous Solid Dispersions from Two-Dimensional Solid-State NMR Spectroscopy. *Molecular Pharmaceutics* 2019, 16, (6), 2579–2589. [PubMed: 31021639]
70. Su Y; Andreas L; Griffin RG Magic Angle Spinning NMR of Proteins: High-Frequency Dynamic Nuclear Polarization and 1H Detection. *Annual Review of Biochemistry* 2015, 84, (1), 465–497.
71. Wu J; Wu L; Wan F; Rantanen J; Cun D; Yang M Effect of thermal and shear stresses in the spray drying process on the stability of siRNA dry powders. *International journal of pharmaceutics* 2019, 566, 32–39. [PubMed: 31077763]
72. Liao X; Krishnamurthy R; Suryanarayanan R Influence of the active pharmaceutical ingredient concentration on the physical state of mannitol—implications in freeze-drying. *Pharmaceutical research* 2005, 22, (11), 1978–1985. [PubMed: 16132343]
73. Maa Y-F; Costantino HR; Nguyen P-A; Hsu CC The effect of operating and formulation variables on the morphology of spray-dried protein particles. *Pharmaceutical development and technology* 1997, 2, (3), 213–223. [PubMed: 9552449]
74. Chew NYK; Shekunov BY; Tong HHY; Chow AHL; Savage C; Wu J; Chan H-K Effect of Amino Acids on the Dispersion of Disodium Cromoglycate Powders. *Journal of Pharmaceutical Sciences* 2005, 94, (10), 2289–2300. [PubMed: 16136546]
75. Mangal S; Nie H; Xu R; Guo R; Cavallaro A; Zemlyanov D; Zhou Q Physico-Chemical Properties, Aerosolization and Dissolution of Co-Spray Dried Azithromycin Particles with L-Leucine for Inhalation. *Pharmaceutical Research* 2018, 35, (2), 28. [PubMed: 29374368]
76. Yu J; Chan H-K; Gengenbach T; Denman JA Protection of hydrophobic amino acids against moisture-induced deterioration in the aerosolization performance of highly hygroscopic spray-dried powders. *European Journal of Pharmaceutics and Biopharmaceutics* 2017, 119, 224–234. [PubMed: 28655664]
77. Mah PT; O'Connell P; Focaroli S; Lundy R; O'Mahony TF; Hastedt JE; Gitlin I; Oscarson S; Fahy JV; Healy AM The use of hydrophobic amino acids in protecting spray dried trehalose formulations against moisture-induced changes. *European Journal of Pharmaceutics and Biopharmaceutics* 2019, 144, 139–153. [PubMed: 31536784]

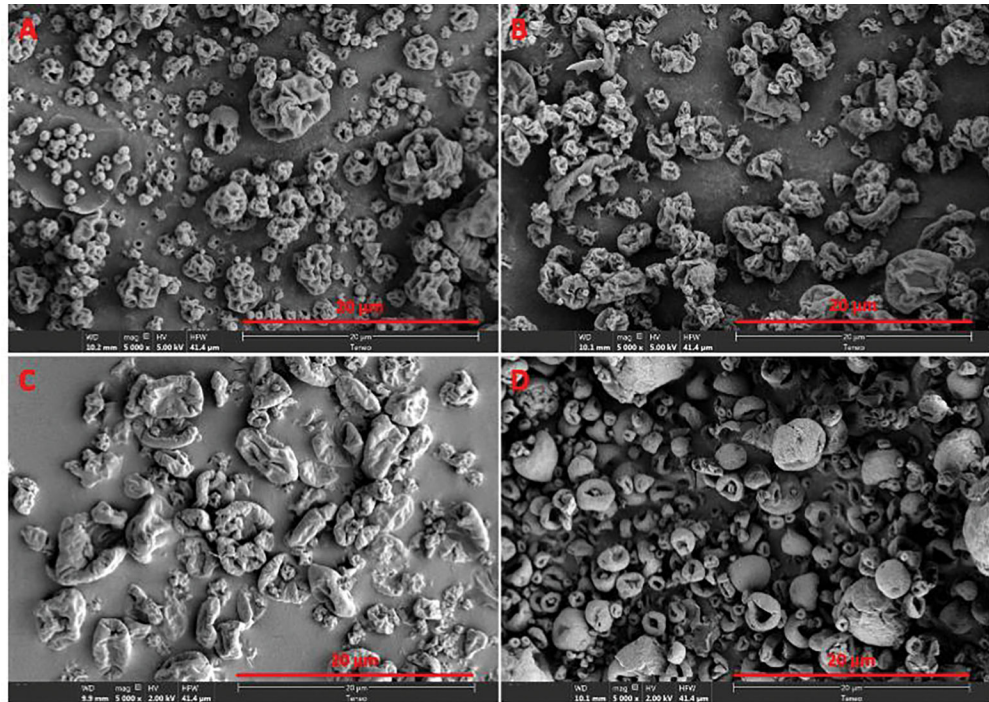


Figure 1. Scanning electron micrographs of spray-dried solids in (A) BSA without excipient; (B) BSA-trehalose formulation; (C) BSA-mannitol formulation; (D) BSA-leucine formulation.

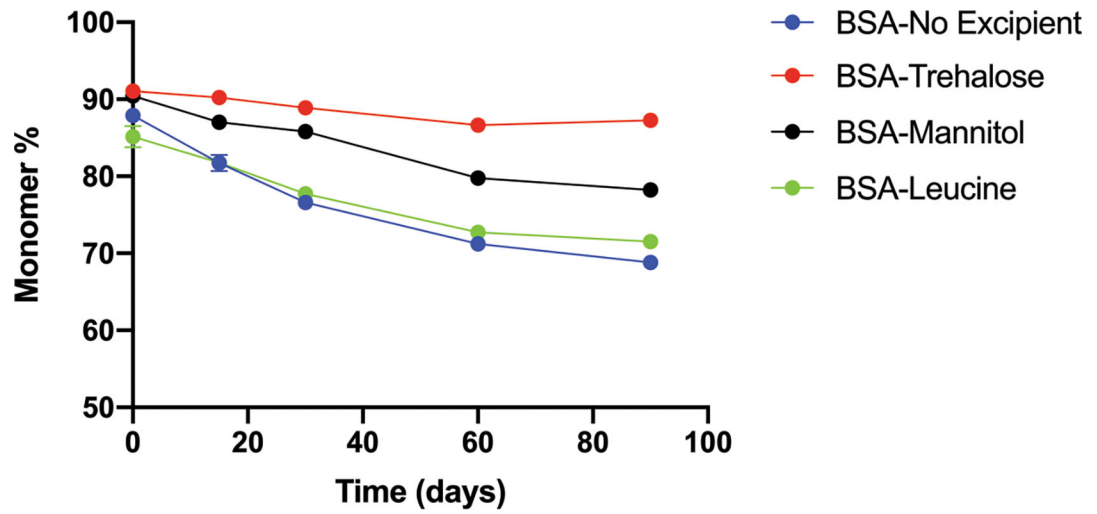


Figure 2. Monomer loss of BSA in the spray-dried solid formulations during the stability study at 40 °C (n = 3, mean ± SD). Error bars smaller than the symbol are not shown.

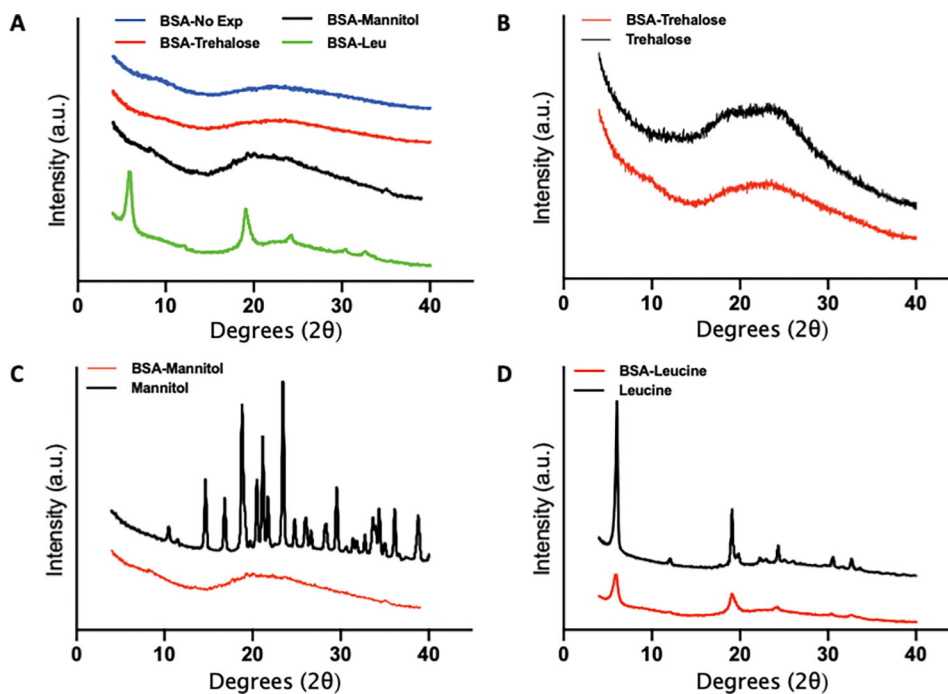


Figure 3. PXRD spectra of the spray-dried BSA formulations and spray-dried excipient references: (A) the spray-dried BSA without excipient, and with trehalose, mannitol or leucine; (B) the spray-dried BSA with trehalose and the spray-dried trehalose; (C) the spray-dried BSA with mannitol and the spray-dried mannitol; (D) the spray-dried BSA with leucine and the spray-dried leucine.

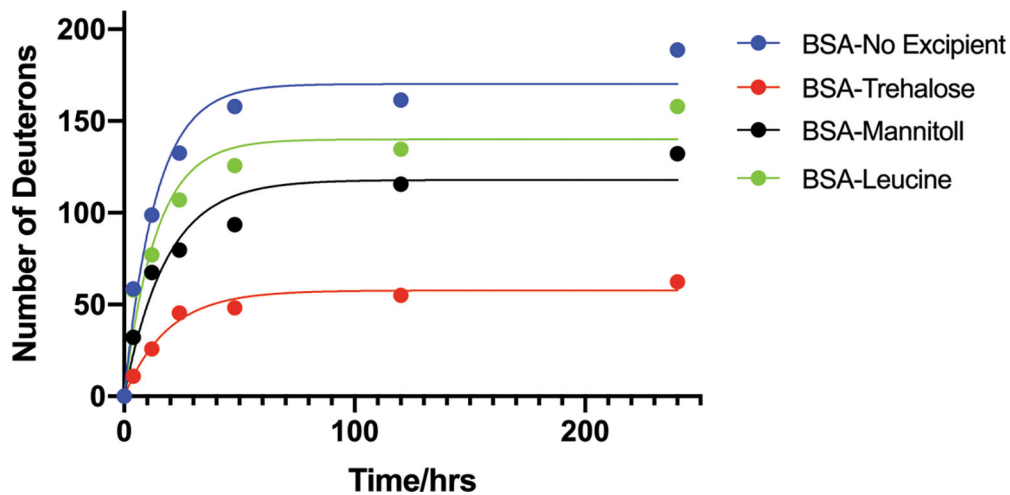


Figure 4. The kinetics of deuterium uptake in the spray-dried solids with D₂O exposure up to 240 h (mean \pm SD, n =3). Lines represent curve fitting to the mono-exponential model (eq. 1). Error bars smaller than the symbol cannot be shown in the graph.

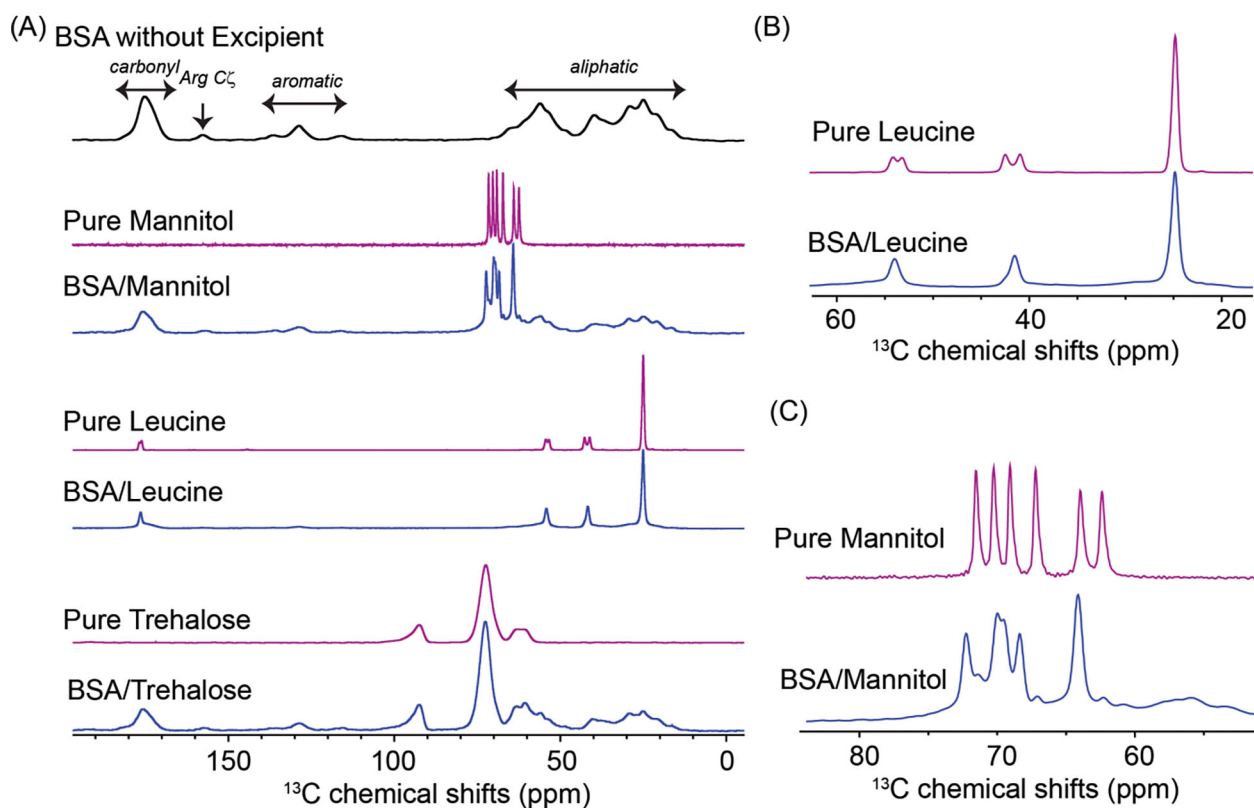


Figure 5. (A) $1D$ 1H - ^{13}C cross-polarization spectra of spray-dried BSA with and without excipients, and the corresponding spray-dried excipient references; (B) detailed spectral comparison of spray-dried leucine reference (magenta) and BSA-leucine (blue); (C) detailed spectral comparison of spray-dried mannitol reference (magenta) and BSA-mannitol (blue).

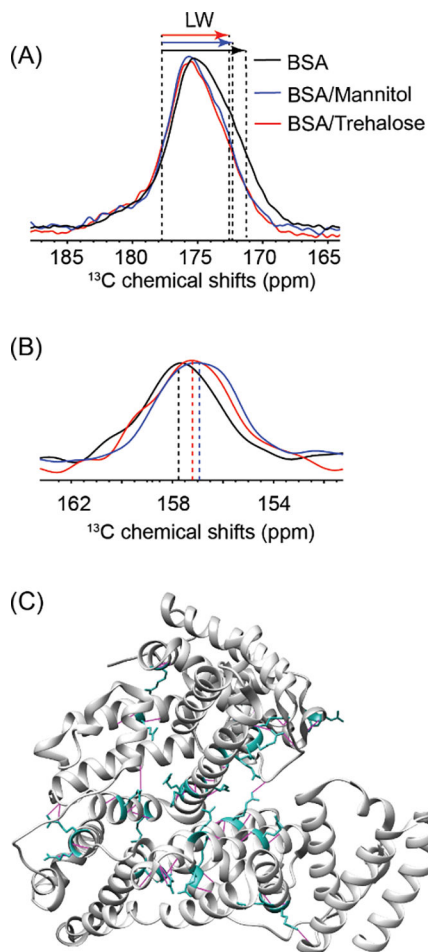


Figure 6. Comparison of the (A) carbonyl region and (B) Arg C_ϵ peaks of spray-dried BSA without any excipient, BSA-mannitol and BSA-trehalose formulation; (C) X-ray crystallography structure of BSA monomer (PDB ID: 4F5S) highlighting the Arg residues (cyan) and hydrogen bonds with other residues to maintain the secondary and tertiary protein structure (magenta).

Table 1.

The moisture content (w/w%) measured by Karl Fischer titration (n = 3, mean \pm SD).

Excipient	Moisture Content (%)
No Excipient	0.7 \pm 0.6
Trehalose	0.3 \pm 0.1
Mannitol	0.3 \pm 0.1
Leucine	0.7 \pm 0.3

Author Manuscript

Author Manuscript

Author Manuscript

Author Manuscript

Table 2.

Non-linear regression parameters of ssHDX kinetic curve fitting

Formulation	D_{max} (Da)	k (h⁻¹)
No Excipient	170.1	0.073
Trehalose	57.7	0.053
Mannitol	117.9	0.054
Leucine	140.0	0.072

Author Manuscript

Author Manuscript

Author Manuscript

Author Manuscript

Table 3.

NMR linewidth and ^1H relaxation parameters of the spray-dried BSA without excipient, BSA-mannitol and BSA-trehalose formulations (mean \pm SD, n =3)

Formulation	Carbonyl Linewidth (LW)/ (Hz)	T_1 (s)			$T_{1\rho}$ (ms)		
		Protein	Excipient	Difference	Protein	Excipient	Difference
BSA	567	1.35 \pm 0.03	-	-	7.37 \pm 0.08	-	-
BSA-Mannitol ^(a)	530	2.21 \pm 0.08	15.94 \pm 2.75	13.73	4.11 \pm 0.22	22.14 \pm 2.85	18.03
BSA-Mannitol ^(b)			2.79 \pm 0.18	0.58		1.39 \pm 0.23	2.72
BSA-Trehalose	501	2.74 \pm 0.08	2.84 \pm 0.06	0.1	9.78 \pm 0.39	9.29 \pm 0.12	0.49

^(a) crystalline form and

^(b) amorphous form of mannitol detected in the BSA-mannitol formulation